Journal of Biomechanics 46 (2013) 1759–1766

Contents lists available at SciVerse ScienceDirect

Journal of Biomechanics

journal homepage: www.elsevier.com/locate/jbiomech
www.JBiomech.com

Local axial compressive mechanical properties of human carotid atherosclerotic plaques—characterisation by indentation test and inverse finite element analysis

Chen-Ket Chai [a,*], Ali C. Akyildiz [b], Lambert Speelman [b,c], Frank J.H. Gijsen [b], Cees W.J. Oomens [a], Marc R.H.M. van Sambeek [d], Aad van der Lugt [e], Frank P.T. Baaijens [a]

[a] Department of Biomedical Engineering, Eindhoven University of Technology, Eindhoven, The Netherlands
[b] Department of Biomedical Engineering, Thoraxcenter, Erasmus Medical Centre, Rotterdam, The Netherlands
[c] Interuniversity Cardiology Institute Netherlands (ICIN), Utrecht, The Netherlands
[d] Catharina Hospital Eindhoven, Eindhoven, The Netherlands
[e] Department of Radiology, Erasmus Medical Centre, Rotterdam, The Netherlands

ARTICLE INFO

Article history:
Accepted 16 March 2013

Keywords:
Atherosclerosis
Plaque rupture
Indentation
Carotid artery
Finite element method

ABSTRACT

The fibrous cap of an atherosclerotic plaque may be prone to rupture if the occurring stresses exceed the strength of the cap. Rupture can cause acute thrombosis and subsequent ischaemic stroke or myocardial infarction. A reliable prediction of the rupture probability is essential for the appropriate treatment of atherosclerosis. Biomechanical models, which compute stresses and strain, are promising to provide a more reliable rupture risk prediction. However, these models require knowledge of the local biomechanical properties of atherosclerotic plaque tissue. For this purpose, we examined human carotid plaques using indentation experiments. The test set-up was mounted on an inverted confocal microscope to visualise the collagen fibre structure during the tests. By using an inverse finite element (FE) approach, and assuming isotropic neo-Hookean behaviour, the corresponding Young's moduli were found in the range from 6 to 891 kPa (median 30 kPa). The results correspond to the values obtained by other research groups who analysed the compressive Young's modulus of atherosclerotic plaques. Collagen rich locations showed to be stiffer than collagen poor locations. No significant differences were found between the Young's moduli of structured and unstructured collagen architectures as specified from confocal collagen data. Insignificant differences between the middle of the fibrous cap, the shoulder regions, and remaining plaque tissue locations indicate that axial, compressive mechanical properties of atherosclerotic plaques are independent of location within the plaque.

1. Introduction

Atherosclerotic plaque rupture is the main cause of ischaemic stroke and myocardial infarction. Plaque rupture can lead to thrombus formation on the disrupted plaque surface and subsequent embolisation of thrombus into the distal vessels or to acute vessel occlusion. Rupture prone plaques are characterised by the presence of inflammatory cells, intraplaque haemorrhage and a lipid rich necrotic core (LRNC) covered by a thin fibrous cap. A reliable prediction model of cap rupture has a big impact on the treatment of atherosclerosis and atherosclerosis-related diseases (Rothwell and Warlow, 1999). Currently, the used methods to estimate plaque rupture is merely based on geometrical parameters, whereas biomechanical models have shown to provide a better risk assessment (Akyildiz et al., 2011; Finet et al., 2004; Hayenga et al., 2011; Salunke and Topoleski, 1997; Tracqui et al., 2011). However, the results of these models strongly depend on material properties of individual plaque components. Therefore, these models will benefit from specific knowledge of material properties of individual plaque components.

Experimental data on the mechanical properties of atherosclerotic tissue are scarce and show large variability, ranging from very soft (30–40 kPa, Lee et al. 1992; Barrett et al., 2009) to very stiff (of order 1 MPa, Lee et al., 1991; Loree et al., 1994; Ebenstein et al., 2002; Holzapfel et al., 2004). Moreover, most of the data represent only the average global stiffness of the plaque tissue tested and do not distinguish between different components within a plaque.

Recently, an experimental technique was developed by Cox et al. (2006, 2008), combining micro-indentation tests on soft

* Correspondence to: Eindhoven University of Technology, Department of Biomedical Engineering, PO Box 513, GEM-Z 4.14, 5600 MB Eindhoven, The Netherlands. Tel.: +31 40 247 5392; fax: +31 40 244 7355.
E-mail addresses: c.chai@tue.nl, chai.chenket@gmail.com (C.-K. Chai).

0021-9290
http://dx.doi.org/10.1016/j.jbiomech.2013.03.017

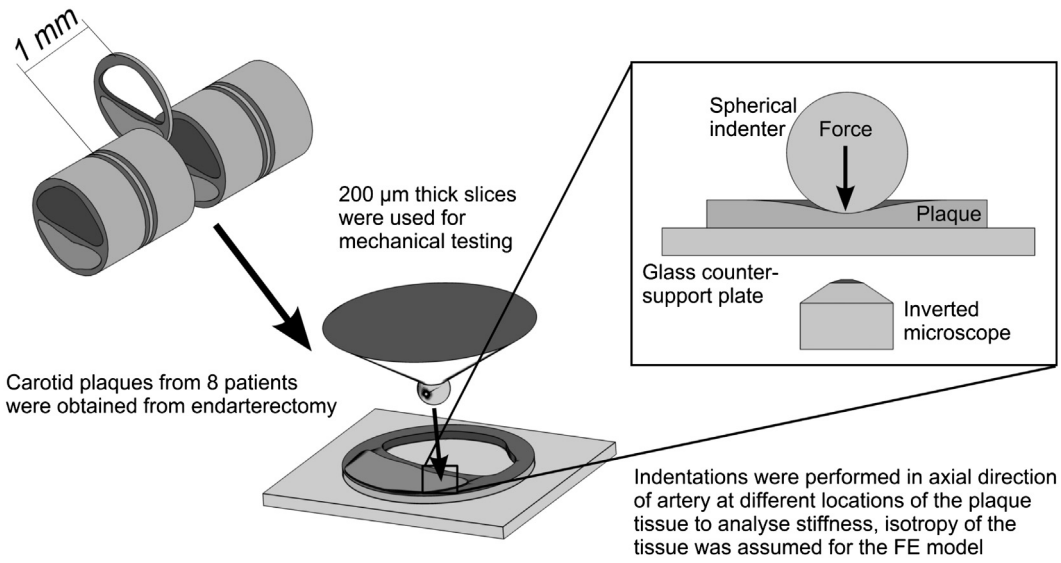

Fig. 1. Sectioning of plaque tissues with a cryotome to create 200 μm thick slices for mechanical testing. Depending on the axial length of the plaque, 6–13 slices were obtained. Adjacent slices are used for histology.

biological materials with confocal laser scanning microscope imaging. We apply this technique to investigate the compressive Young's moduli of different plaque components in the axial direction.

2. Methods

2.1. Preparing plaque tissue

Eight carotid artery endarterectomy specimens were obtained from eight symptomatic patients (2 female, 6 male, age 59 to 87). All plaques had ≥70% stenosis and low calcium content on preoperative CT angiography. Approval was given by the Institutional Review Board of the Erasmus MC, and informed consent was obtained. The plaques were snap-frozen, using liquid nitrogen and stored at −80°C. In a later stage, the plaques were sectioned, using a Leica cryotome at −20°C. Slices of 200 μm thicknesses were obtained with 1 mm spacing in between for the indentation experiments (Fig. 1).

Distal and proximal to each test section, slices of 5 μm thickness were cut for histology. A Gomori trichrome staining was applied on these slices. This stains collagen green/blue, muscle cells red, and nuclei black/blue. The histological images were used to determine indentation locations by visual registration before the experiments.

Prior to the mechanical testing, the 200 μm thick sections were thawed to room temperature and stained overnight using a fluorescent CNA35-OG488 probe (Nash-Krahn et al., 2006). This fluorescent staining was applied to visualise the collagen architecture of the plaque tissue.

2.2. Indentation test and imaging

To analyse the local mechanical properties of a plaque tissue, an existing indentation test set-up (Cox et al., 2008) was adapted, using a surface force apparatus developed by Vaenkatesan et al. (2006). At each testing location at least three consecutive indentations were performed using a spherical indenter with a diameter of 2 mm. During indentation the force response and the indentation depth were recorded. As described in Cox et al. (2010), the first indentation was considered as preconditioning and these results were not included. The measurements at the same indentation location were averaged. An inverted confocal laser scanning microscope (magnification 10x, excitation 488 nm, emission 500 nm high-pass), located underneath the set-up, was used to visualise the collagen structure, which were fluorescently stained (Fig. 1 and 2, Nash-Krahn et al., 2006; Boerboom et al., 2007). More detailed information regarding the indentation set-up can be found in Cox et al. (2005).

2.3. Data analysis

A 3D finite element model was created to simulate the indentation experiments, as previously described by Cox et al. (2008). The behaviour of the tissue was described with an isotropic incompressible Neo-Hookean model. The local shear modulus G at the test location was estimated by fitting the model to the experimental force-indentation-depth curve. The force response of up to 30% indentation of the tissue thickness was used for the parameter identification (Fig. 3). Simulations confirmed that the circumferential strain at 30% indentation of tissue thickness was about 20%, which corresponds to the upper limit of physiological strain range. The contact radius between indenter and tissue was about 0.4 mm². To fit the experimental data with the simulated data, the least-square method was used. To compare the results obtained in this study with the results in literature the Young's modulus E was calculated from the shear modulus G with

$$E = 3G \tag{1}$$

Measurement positions were classified by their indentation location and collagen structure. Based on the collagen structure, three different types of collagen architectures were distinguished using the confocal microscope (Fig. 2). Following the approach of Timmins et al. (2010) and Ng and Swartz (2006), a customised MATLAB script was generated to estimate the alignment index (AI) of the collagen fibres. The AI was given by

$$AI = \frac{\delta/(\Delta+\delta)}{\delta_{IR}/(\Delta+\delta)_{IR}} = \frac{\delta/(\Delta+\delta)}{40/180}, \tag{2}$$

where δ described the sum of frequencies of fibres within $\pm 20^\circ$ of the preferred fibre alignment (PFA) and Δ was the sum of frequencies of the remaining fibres outside of this range. The sums of frequencies δ_{IR} and Δ_{IR} described the corresponding sum of frequencies for an ideal random (IR) distribution, where the fibre dispersion is isotropic. These sum of frequencies were per definition $\delta_{IR}=40$ and $\Delta_{IR}=140$.

To decide if the collagen distribution was structured or unstructured an arbitrary threshold of $AI=1.4$ was chosen. Therefore, locations which showed a high amount of collagen fibres with a clear alignment ($AI > 1.4$) of the fibres were classified as dense structured collagen areas (SC). Positions with high amounts of collagen, but no clear alignment of the fibres ($AI < 1.4$), were characterised as loose unstructured collagen locations (UC). Collagen poor areas, primarily in the lipid rich necrotic core (LRNC) region, were classified as CP.

Each slice was indented at one to eight different locations. The locations were classified as middle of the fibrous cap, shoulder region of the fibrous cap, lipid rich necrotic core (LRNC) region and intima (remaining arterial wall regions, Fig. 4).

After the measurements the homogeneity at the tissue testing locations were examined based on the confocal images. Two observers (CKC and ACA), who were blinded to the stiffness results, conducted this evaluation. The following criteria led to the exclusion of the results from further analysis:

- Presence of debris or other foreign material, which were not identified as collagen fibres.
- Ruptured collagen fibres.
- Gap in the tissue which did not correspond to the structure of the surrounding tissue.
- Folded tissue, which can lead to slipping of the tissue influencing the stiffness results.

Statistical analysis was conducted to compare stiffness between indentation locations and between collagen types. The stiffness results showed a non-Gaussian

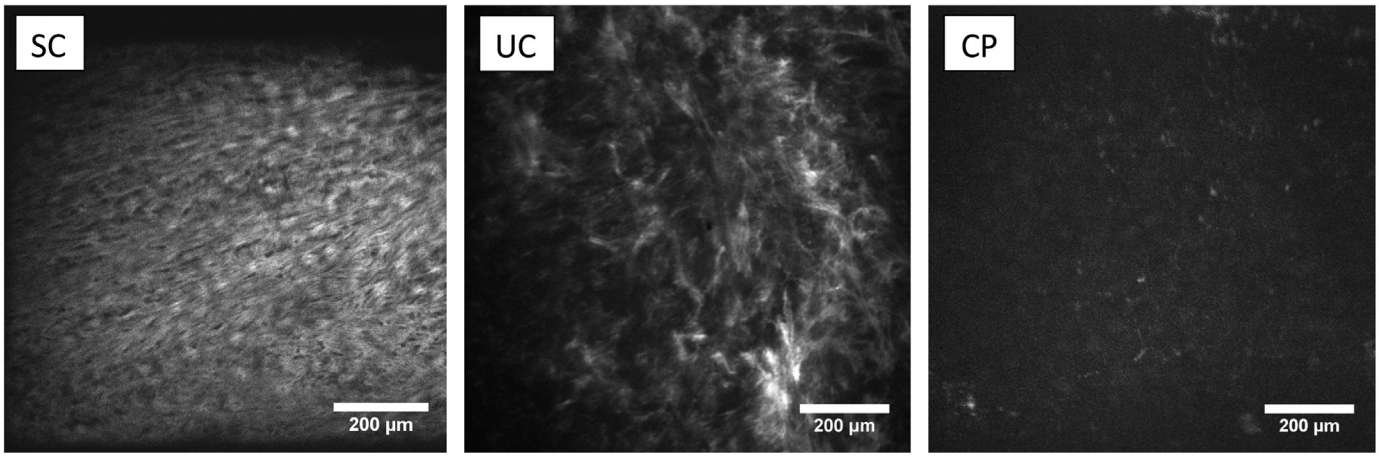

Fig. 2. Examples of a dense structured collagen location (SC), a loose unstructured collagen location (UC) and a collagen poor location (CP).

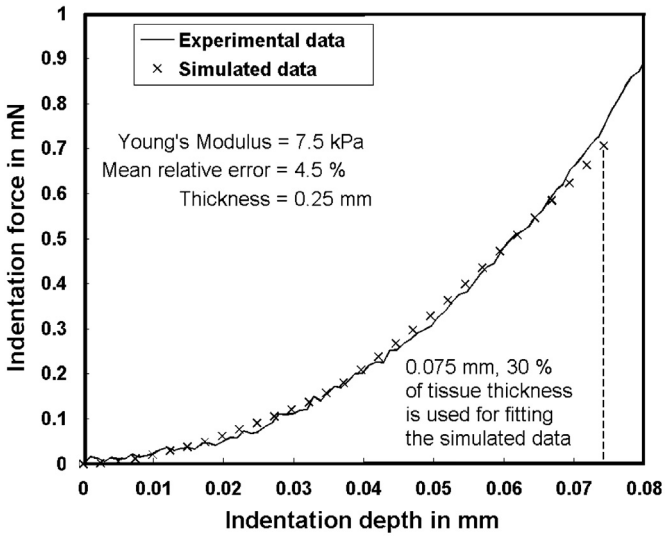

Fig. 3. A least-square method was used to fit a neo-Hookean material model to the experimental force-indentation data, 30% of the tissue thickness is indented and used for fitting to simulated data (here: 0.075 mm).

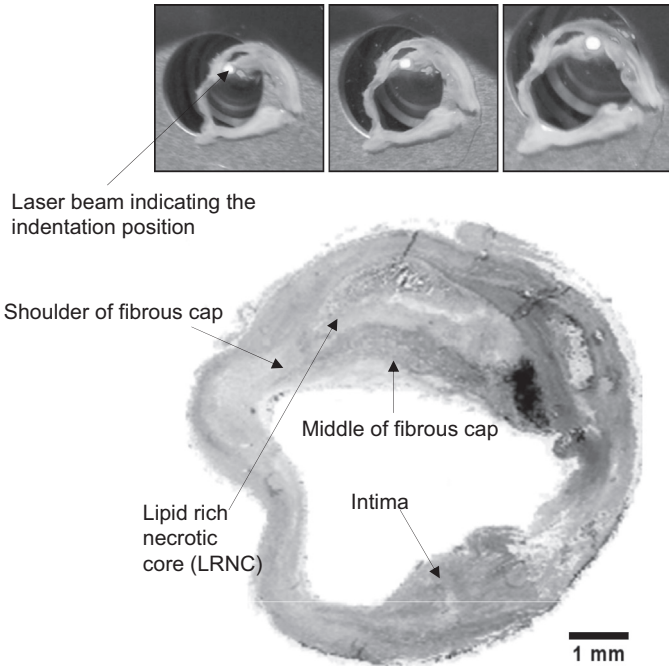

Fig. 4. Histological slice (bottom). The top figures show the indentation positions indicated by the laser beam.

distribution. The Kruskal–Wallis test (Dunn procedure) was applied using GraphPad Prism version 5.04 for Windows. A p-value <0.05 was considered as significant result.

3. Results

3.1. Representative plaque result

In total, eight human carotid plaques were tested. Depending on the length of the plaque, 6–13 slices were obtained per plaque. At 284 locations, 574 measurements were performed. After examining the confocal images for homogeneity of test locations, 214 locations were used for further analysis. The average thickness of the tested plaque sections was 240 μm ($\pm$80 μm).

Representative results of one plaque are shown in Fig. 5. On the left-hand side of Fig. 5, a schematic representation of the plaque is shown where the common carotid artery bifurcates into internal (ICA) and external carotid artery (ECA). Among 9 slices obtained from the plaque, the most 3 proximal slices (slice 7–9 in Fig. 5) contained both the internal and the external artery. The other slices only included the internal carotid artery. Above the illustration of the bifurcation, a schematic image of a slice is shown, where the different coloured areas represent the indentation locations. On the right-hand side of Fig. 5, a table shows the Young's moduli in kPa. Corresponding to the schematic image of the slice, the different coloured columns represent the indentation locations. The collagen rich fibrous cap and intima locations, where further divided into dense structured collagen (SC) and loose unstructured collagen (UC). LRNC locations were collagen poor (CP). At slice 1–4 and at slice 6 a single location in the middle of the cap was measured. Slice 5 had a fibrous cap large enough to perform indentation tests at two different middle cap locations. Each value in the table represents the average of at least two consecutive measurements at the same location. For the middle of the cap all values were in the range from 15 to 53 kPa with an average of 41 kPa and standard deviation (SD) of 12 kPa. Moreover, based on the collagen dispersion, only SC regions were found in the middle of the cap. Most of the indentation locations at the shoulder of the cap were also found to be SC regions. Only at slice 2 and 8 UC regions were present. The Young's modulus of the shoulder regions ranged from 23 to 104 kPa. For this location the average value was 43 kPa, similar to the middle of the cap. At the intima regions, five SC and three UC locations were found.

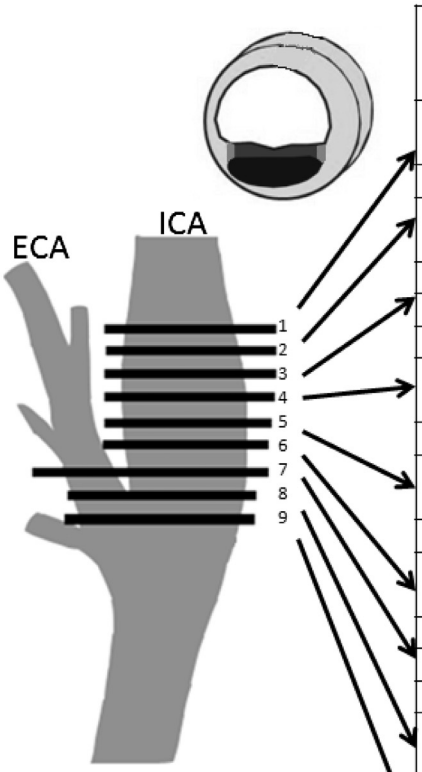

Slice	Middle cap SC	Middle cap UC	Shoulder cap SC	Shoulder cap UC	Intima SC	Intima UC	LRNC CP	Average (SD) of fibrous cap in kPa
1	52		43 37					34 (11)
2	15			36		94 114		
3	34		23					
4	45		29 51		7			40 (9)
5	53 42		30		57			
6	44		34 31					
7			104			33		69 (27)
8				65 37	51		18	
9					20 64			
Average (SD) in kPa	41 (12)		42 (23)	46 (13)	40 (22)	80 (34)	18 (0)	

Fig. 5. Left: Schema of a carotid plaque at the bifurcation of common carotid into internal (ICA) and external carotid artery (ECA), Right: Young's moduli in kPa for this plaque, SC (dense structured collagen), UC (loose unstructured collagen) and CP (collagen poor), LRNC (lipid rich necrotic core).

The Young's moduli varied from 7 to 114 kPa with an average of 40 kPa for SC and 80 kPa for UC. For this plaque only one CP location with a Young's modulus of 18 kPa was available for testing. To investigate the difference of mechanical properties in the longitudinal direction of a vessel, plaques were divided into three parts each consisting of three slices representing proximal, middle and distal regions of the plaque. This last column of the table shows the average values and the standard deviation of these three regions. For this particular plaque the proximal region is stiffer than the distal region.

3.2. Collagen structure

There were 119 positions classified as SC, 75 positions as UC, and 20 positions as CP areas. No significant differences could be found between the collagen rich location SC and UC (Fig. 6). The collagen rich locations showed a high variation of stiffness results, ranging from 6 to 891 kPa. However, CP areas had a smaller range (9–143 kPa), and the results were significantly lower (median 16 kPa) compared to the collagen rich locations SC (median 31 kPa) and UC (median 33 kPa) (Fig. 6).

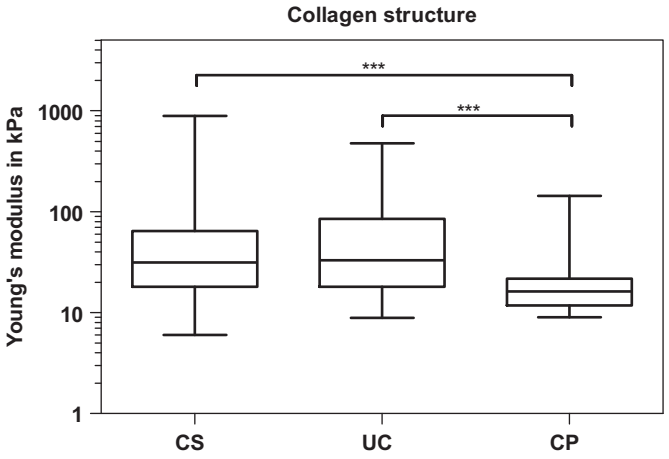

Fig. 6. Box and whisker plots (minimum–maximum) of the Young's moduli, structured (SC), unstructured (UC) and collagen poor areas (CP), ***p-value < 0.001.

3.3. Indentation locations

Based on the histology images, indentation locations were chosen before performing the experiments. There were 43 indentation locations identified as middle of the fibrous cap, 61 as shoulder regions of the cap, 90 indentation locations as intima, and 20 as LRNC.

Table 1 summarises the results of all plaques tested. In Fig. 7, the logarithmic scaled y-axis displays the Young's modulus in kPa, the x-axis shows the indentation location, middle of cap (median = 31 kPa), shoulder of cap (median = 27 kPa), intima (median = 46 kPa), and LRNC locations (median = 16 kPa). It was found

Table 1
Summary of indentation test results, Mid—Middle of fibrous cap, Sh—Shoulder of cap.

	SC/Mid	SC/Sh	SC/Intima	UC/Mid	UC/Sh	UC/Intima	CP/LRNC
No. of test locations	29	36	54	14	25	36	20
Minimum in kPa	12	6	6	11	9	11	9
25% Percentile in kPa	18	18	17	14	15	30	12
Median in kPa	36	26	35	28	27	58	16
75% Percentile in kPa	54	43	95	34	46	109	22
Maximum in kPa	891	182	305	166	203	475	143

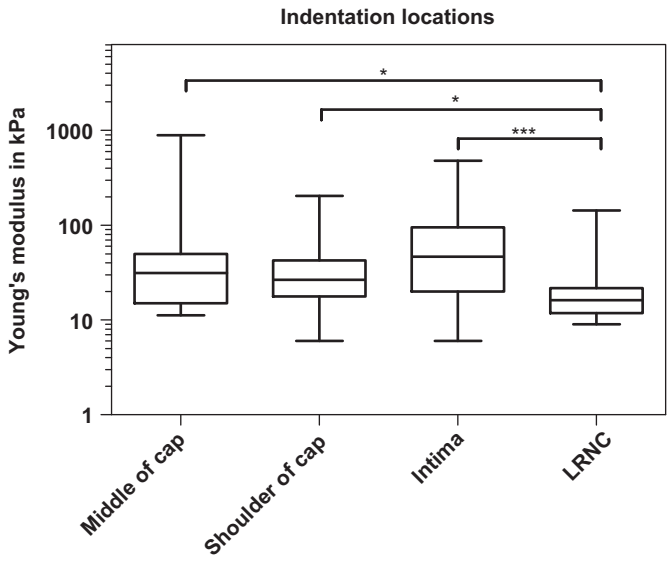

Fig. 7. Box and whisker plots (minimum-maximum) of the Young's moduli of the different indentation locations and the significance of the values compared to each other, * p-value < 0.05, *** p-value < 0.001.

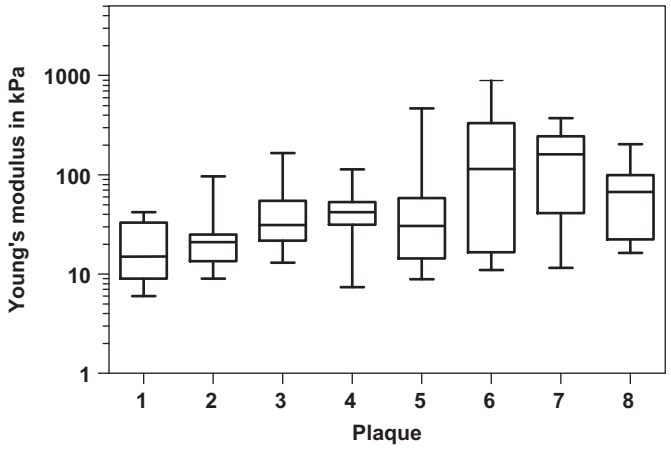

Fig. 8. Box and whisker plots (minimum–maximum) of the Young's moduli of 8 human carotid atherosclerotic plaques, excluding collagen poor locations.

that the fibrous cap and intima regions are significantly stiffer than the LRNC regions. No differences were observed between the middle and shoulder of cap, and the intima locations.

3.4. Inter- and intra-plaque variability, comparison between longitudinal and transversal slices, and change of mechanical properties in longitudinal direction

The axial compressive Young's modulus of each plaque, excluding the collagen poor locations, are summarised in Fig. 8. The results show that there is a large variation in Young's moduli within each plaque, especially for plaque 6 (11–891 kPa). Due to this variation, no significant differences between plaques were observed.

The indentation tests were performed in axial direction of the artery on transversal slices. For one plaque, part of the tissue was sliced in the longitudinal direction and these longitudinal slices were used for testing. The resulting Young's moduli show no significant differences between the transversal and longitudinal slices (data not shown).

From proximal to distal, the results indicated no significant differences in Young's modulus. In three atherosclerotic plaques the fibrous cap at the proximal region showed higher stiffness than the distal region. However, in two cases the proximal site was softer than the distal side. For the remaining three plaques, numbers of indentation locations at the fibrous cap were not sufficient to make a comparison between proximal and distal regions.

4. Discussions

In this study we used an indentation test and inverse FE analysis to estimate the compressive Young's moduli of carotid atherosclerotic plaque tissue in axial direction. Assuming isotropic neo-Hookean behaviour, the Young's moduli were found in the range from 6 kPa to 891 kPa (median of 30 kPa) corresponding to values found in the literature. Collagen poor regions were softer than collagen rich locations. However, no significant differences were observed between the Young's moduli of structured and unstructured collagen architectures. Moreover, no significant differences were found between the middle of the fibrous cap, the shoulder regions, and remaining intima locations. Therefore, the results indicate that the macroscopic behaviour of carotid atherosclerotic fibrous plaque tissue can be approximated by a single material model. However, it should be noted that the sample size (8 endarterectomy specimens) may not be sufficiently large to detect a statistical difference between the middle and shoulder regions of the fibrous cap, particularly since other patient-specific variables (age, gender, etc.) had not been controlled for.

A literature review revealed that there is a high variability of stiffness values of plaque tissue (Lee et al., 1991; Lee et al., 1992; Loree et al., 1994; Loree et al., 1994a; Beattie et al., 1998; De Korte et al., 2000; Kanai et al., 2003; Holzapfel et al., 2004; Barrett et al., 2009). Our results are in the lower region of the range reported in literature and are consistent with the values obtained by Lee et al. (1992) and Barrett et al. (2009) (Table 2). However, our results differ from the values obtained by other groups (Lee et al., 1991; Loree et al., 1994; Loree et al., 1994a; Beattie et al., 1998; De Korte et al., 2000; Kanai et al., 2003; Holzapfel et al., 2004). Possible explanations for this might be the different methods used to measure the mechanical properties of atherosclerotic plaque tissue which lead to the measurement of different Young's moduli (Table 2). In addition, the direction of measured stiffness also plays

Table 2
Measured Young's moduli (in kPa) for atherosclerotic plaque tissue.

	Specimen type	Test method	Classification		
			Cellular		Hypocellular
Lee et al. (1991)	Abdominal aorta	Radial compression, dynamic, values at 1 Hz	510 ± 220 ($n=7$)		900 ± 220 ($n=9$)
Loree et al. (1994)	Abdominal/thoratic aorta	Circumferential tension, static creep type test	927 ± 468 ($n=12$)		2312 ± 2180 ($n=9$)
			Non-fibrous		Fibrous
Lee et al. (1992)	Abdominal aorta	Radial compression, static creep type test and ultrasound	41 ± 19 ($n=14$)		82 ± 33 ($n=18$)
Beattie et al. (1998)	Aorta	Bi-linear isotropic	4, strain $<18\%$ 39, strain $>18\%$		483, strain $<8.2\%$ 1820, strain >8.2
De Korte et al. (2000)	Femoral/coronary arteries	Incremental pressure–strain	222 ($n=13$)		493 ($n=62$)
Ebenstein et al. (2002)	Carotid artery	Radial nano-indentation and FTIR	620 (60–4900)		1500 (100–21500)
Kanai et al. (2003)	Iliac artery	Circumferential incremental with transcutaneous ultrasound	81 ± 40 ($n=9$)		1000 ± 630 ($n=9$)
Holzapfel et al. (2004)	Iliac artery	Axial and circumferential tension	–		Axial, 1200 Circum, 840 ($n=107$)
Barrett et al. (2009)	Carotid artery	Radial indentation and inverse FE analysis	–		33 (21–300, $n=8$)
			Collagen poor		Collagen rich
Current study	Carotid artery	Axial indentation and inverse FE analysis	16 (9–143)		32 (6–891)
			Middle Cap	Shoulder Cap	Intima
			31 (11–891)	27 (6–203)	46 (6–475)

a role. The anisotropy of the tissue suggests that testing the stiffness of plaque tissue in different directions will lead to different results, although our values obtained from testing a small set of longitudinal slices were comparable to the results we obtained for transversal slices. Furthermore, different values might be the result of the measurements of different specimen types. Since the geometry of arteries at different locations varies and arteries from various locations experience different stresses and strains, it is suggested that the biomechanical properties of arteries from different location also vary. Differences between the values we obtained and the results of the other research groups might be also caused by the various methods used to classify the tissue. In our study we distinguish between collagen structure and between different plaque locations.

Measurements at same indentation positions led to a mean difference of 12% ($\pm 14\%$) showing that the indentation test method itself is reproducible. Taking the 25% and 75% percentile as range, the variability is similar to the range obtained by Barrett et al. (2009) and Lee et al. (1992). It is smaller than the variability obtained by other research groups (Loree et al., 1994; Beattie et al., 1998; Ebenstein et al., 2002). Since the range of values we found is similar for each plaque we tested and this is also observed by most research groups, the obtained range must reflect the variable nature of the mechanical properties of biological tissue.

It is suggested that, due to the different shear stress between the proximal and distal regions, different plaque morphology and therefore different stiffness results in those regions of the plaque can be expected (Dirksen et al., 1998; Slager et al., 2005; Gijsen et al., 2008). Gijsen et al. (2008) showed on human coronary arteries that the shear stress upstream is significantly higher than downstream. Dirksen et al. (1998) found a significant difference between the cell compositions of proximal and distal parts of carotid plaques. Therefore, the results from literature suggest that also the stiffness of the fibrous cap proximal and distal of a plaque could be different. Using plaque tissue from carotid endarterectomy patients, it was possible to analyse the changes of stiffness from proximal to distal locations in five samples. No significant differences could be observed.

To analyse the influence of the collagen structure on the mechanical properties a confocal microscope was used to identify the collagen structure of the tested tissue location. The results show a wide spread of mechanical properties between plaques. Stiffness values of collagen poor locations, which are mostly found in the LRNC, have less variation than collagen rich regions. A statistical analysis using a non-parametric approach indicated that the collagen rich locations (structured and unstructured) are significantly stiffer than collagen poor locations. For collagen rich positions, no significant differences are found between the different collagen structures, suggesting that the architecture of collagen has no obvious effect on the Young's modulus. It is surprising that our results show no influence of the collagen structure on the stiffness results. Reasons for this might be the use of an isotropic model assuming homogeneity of the sample which might not reflect the actual mechanical behaviour of the tissue. In addition, it has to be noted that not only the collagen structure but also the amount of collagen influences the stiffness of the plaque tissue. The quantity of collagen was not measured during this study. Burleigh et al. (1992) showed that plaque caps seem to require more quantities of collagen than neighbouring intima to maintain the same mechanical strength indicating that the collagen structure in the cap is less efficiently organised than in adjunct intima. The result of Burleigh et al. (1992) suggests that for the stiffness of plaque caps the amount of collagen play a bigger role rather than the collagen structure. Therefore, the last point is probably the main reason why we could not observe a significant difference between structured and unstructured collagen fibres.

For different indentation locations of single slices, it is observed that the fibrous cap tissue and intima tissue are significantly stiffer than the collagen poor regions which could be expected. However, no differences were found between the middle parts of the cap tissue, shoulder regions of the cap, and intima positions suggesting

that one material model can be used to approximate the diseased intima and fibrous cap. On the other hand, considering the high variability of results, it is clear that finding a significant tendency is difficult.

A limitation of the study is the fact that the samples were frozen for logistical reasons. According to Schaar et al. (2002), the influence of freezing on the mechanical properties of coronary arteries plays only a limited role. The freezing protocol applied in this study included dipping the sample in liquid nitrogen for snap freezing. This procedure is widely used to avoid ice-crystal formation. Hemmasizadeh et al. (2012) used nano-indentation to show that snap-freezing and storage at −80°C had no significant influence on the mechanical properties of porcine aortas. Therefore, the probability of damage of the collagen fibres due to ice-crystal formation was minimised. Furthermore, the indentation tests were performed at least twice at the same indentation location and the results were reproducible indicating that no damage to the tissue architecture occurred. The measurements were controlled by confocal microscopic visualisation and also no damage to the tissue was observed. Moreover, the histological data was examined and indicated that no damage due to ice-crystallisation was present.

In literature the mechanical properties of atherosclerotic plaques are usually given only as Young's moduli. Furthermore, it is not always clear whether or not this is a Young's modulus determined at small strains, or a secant modulus of the slope of a curve at a certain strain level. Considering these reservations, the obtained values from this study were compared to the results in literature using $E=3G$, which is only valid at small strains.

The values of the lipid core regions appear to be higher than previously reported data (Cheng et al., 1993). A possible explanation might be that the mechanical tests were performed at room temperature. Testing at this temperature might affect the values for lipid core regions. The physiological mechanical properties of the lipid rich necrotic core at body temperature might be very different from their mechanical properties at room temperature. Therefore, these results should be dealt with caution when including them in simulations, since this may have a strong impact on the biomechanical stress analysis of plaques (Tang et al., 2005).

In conclusion, the system proved to be suitable to measure the local mechanical properties of plaque tissue. The compressive mechanical properties of human plaques in axial direction are lower than previously reported. Mechanical testing of fibrous cap tissue and surrounding intima tissue showed similar mechanical properties between these locations. They are significantly stiffer than collagen poor regions.

Conflict of interest

We declare that there are no issues that may be considered as potential conflicts of interest to this work.

Acknowledgements

This research was supported by the Centre for Translational Molecular Medicine and the Dutch Heart Foundation (PARISk). The assistance of Kim van Gaalen at the Erasmus Medical Centre is gratefully acknowledged.

References

Akyildiz, A.C., Speelman, L., Van Brummelen, H., Gutiérrez, M.A., Virmani, R., Van der Lugt, A., Van der Steen, A.F.W., Wentzel, J.J., Gijsen, F.J.H., 2011. Effects of intima stiffness and plaque morphology on peak cap stress. BioMedical Engineering OnLine 10 (25), 1–13.

Barrett, S.R.H., Sutcliffe, M.P.F, Howarth, S., Li, Z.-Y., Gillard, J.H., 2009. Experimental measurement of the mechanical properties of carotid atherothrombotic plaque fibrous cap. Journal of Biomechanics 42, 1650–1655.

Beattie, D., Xu, C., Vito, R., Glagov, S., Whang, M.C., 1998. Mechanical analysis of heterogeneous, atherosclerotic human aorta. Journal of Biomechanical Engineering 120, 602–607.

Boerboom, R.A., Nash-Krahn, K., Megens, R.T.A., van Zandvoort, M.A.M.J., Merkx, M., Bouten, C.V.C., 2007. High resolution imaging of collagen organisation and synthesis using a versatile collagen specific probe. Journal of Structural Biology 159, 392–399.

Burleigh, M.C., Briggs, A.D., Lendon, C.L., Davies, M.J., Born, G.V.R., Richardson, P.D., 1992. Collagen type I and III, collagen content, GAGs and mechanical strength of human atherosclerotic plaque caps: span-wise variations. Atherosclerosis 96, 71–81.

Cheng, G.C., Loree, H.M., Kamm, R.D., Fishbein, M.C., Lee, R.T., 1993. Distribution of circumferential stress in ruptured and stable atherosclerotic lesions a structural analysis with histopathological correlation. Circulation 87, 1179–1187.

Cox, M.A.J., Driessen, N.J.B., Bouten, C.V.C., Baaijens, F.P.T., 2005. Mechanical characterization of anisotropic planar biological soft tissues using large indentation: an experimental validation study. In: Rodrigues, H., Cerrolaza, M., Doblare, M., Ambrosio, J., Viceconti, M. (Eds.), Proceedings of ICCB 2005, Lisbon, Portugal. pp. 339–350.

Cox, M.A.J., Driessen, N.J.B., Bouten, C.V.C., Baaijens, F.P.T., 2006. Mechanical characterization of anisotropic planar biological soft tissues using large indentation: a computational feasibility study. Journal of Biomechanical Engineering 128, 428–436.

Cox, M.A.J., Driessen, N.J.B., Boerbom, R.A., Bouten, C.V.C., Baaijens, F.P.T., 2008. Mechanical characterization of anisotropic planar biological soft tissues using finite indentation: experimental feasibility. Journal of Biomechanics 41, 422–429.

Cox, M.A.J., Kortsmit, J., Driessen, N.J.B., Bouten, C.V.C., Baaijens, F.P.T., 2010. Tissue-engineered heart valves develop native-like collagen fiber architecture. Tissue Engineering: Part A 16 (5), 1527–1537.

De Korte, C.L., Pasterkamp, G., Van der Steen, A.F.W., Woutman, H.A., Bom, N., 2000. Characterization of plaque components with intravascular ultrasound elastography in human femoral and coronary arteries in vitro. Circulation 102, 617–623.

Dirksen, M.T., van der Waal, A.C., van den Berg, F.M., van der Loos, C.M., Becker, A.E., 1998. Distribution of Inflammatory cells in atherosclerotic plaques relates to the direction of flow. Circulation 98, 2000–2003.

Ebenstein, D.M. Chapman, J.M. Li, L. Saloner, D. Rapp, J. Pruitt, L.A., 2002. Assessing structure–property relations of diseased tissues using nanoindentation and FTIR. In: Moss, S., (Ed.), Advanced Biomaterials: Characterization, Tissue Engineering, and Complexity, Symposium, Boston: Mat. Res. Soc. pp. 47–52.

Finet, G., Ohayon, J., Rioufol, G., 2004. Biomechanical interaction between cap thickness, lipid core composition and blood pressure in vulnerable coronary plaque: impact on stability or instability. Coronary Artery Disease 15, 13–20.

Gijsen, F.J.H., Wentzel, J.J., Thury, A., Mastik, F., Schaar, J.A., Schuursbiers, J.C.H., Slager, C.J., van der Giessen, W.J., de Feyter, P.J., van der Steen, A.F.W., Serruys, P. W., 2008. Strain distribution over plaques in human coronary arteries relates to shear stress. American Journal of Physiology 295, H1608–H1614.

Hayenga, H.N., Trache, A., Trzeciakowski, J., Humphrey, J.D., 2011. Regional atherosclerotic plaque properties in ApoE−/−Mice quantified by atomic force, immunofluorescence, and light microscopy. Journal of Vascular Research 48, 495–504.

Hemmasizadeh, A., Darvish, K., Autieri, M., 2012. Characterization of changes to the mechanical properties of arteries due to cold storage using nanoindentation tests. Annals of Biomedical Engineering 40 (7), 1434–1442.

Holzapfel, G.A., Sommer, G., Regitnig, P., 2004. Anisotropic mechanical properties of tissue components in human atherosclerotic plaques. Journal of Biomechanical Engineering 126, 657–665.

Kanai, H., Hasegawa, H., Ichiki, M., Tezuka, F., Koiwa, Y., 2003. Elasticity imaging of atheroma with transcutaneous ultrasound: preliminary study. Circulation 107, 3018–3021.

Nash-Krahn, K., Bouten, C.V.C., Van Tuijl, S., Van Zandvoort, M.A.M.J., Merkx, M., 2006. Fluorescently labeled collagen binding proteins allow specific visualization of collagen in tissues and live cell culture. Analytical Biochemistry 350, 177–185.

Lee, R.T., Grodzinsky, A.J., Frank, E.H., Kamm, R.D., Schoen, F.J., 1991. Structure-dependent dynamic mechanical behavior of fibrous caps from human atherosclerotic plaques. Circulation 83 (5), 1764–1770.

Lee, R.T., Richardson, S.G., Loree, H.M., Grodzinsky, A.J., Gharib, S.A., Schoen, F.J., Pandian, N., 1992. Prediction of mechanical properties of human atherosclerotic tissue by high-frequency intravascular ultrasound imaging an in vitro study. Arteriosclerosis, Thrombosis, and Vascular Biology 12, 1–5.

Loree, H.M., Grodzinsky, A.J., Park, S.Y., Gibson, L.J., Lee, R.T., 1994. Static circumferential tangential modulus of human atherosclerotic tissue. Journal of Biomechanics 27 (2), 195–204.

Loree, H.M., Tobias, B.J., Gibson, L.J., Kamm, R.D., Small, D.M., Lee, R.T., 1994a. Mechanical properties of model atherosclerotic lesion lipid pools. Arteriosclerosis, Thrombosis, and Vascular Biology 14, 230–234.

Ng, C.P., Swartz, M.A., 2006. Mechanisms of interstitial flow-induced remodeling of fibroblast–collagen cultures. Annals of Biomedical Engineering 34 (3), 446–454.

Rothwell, P.M., Warlow, C.P., 1999. Prediction of benefit from endarterectomy in individual patients: a risk-modelling study. The Lancet 353, 2105–2110.

Salunke, N.V., Topoleski, L.D.T., 1997. Biomechanics of atherosclerotic plaque. Critical Reviews in Biomedical Engineering 25 (3), 243–285.
Schaar, J.A., de Korte, C.L., Mastik, F., van der Steen, A.F.W., 2002. Effect of temperature and freezing on intravascular elastography. Ultrasonics 40, 879–881.
Slager, C.J., Wentzel, J.J., Gijsen, F.J.H., Thury, A., van der Wal, A.C., Schaar, J.A., Serruys, P.W., 2005. The role of shear stress in the stabilization of vulnerable plaques and related therapeutic implications. Nature Clinical Practice Cardiovascular Medicine 2, 456–464.
Tang, D., Yang, C., Zheng, J., Woodrad, P.K., Saffiz, J.E., Sicard, G.A., Pilgram, T.K., Yuan, C., 2005. Quantifying effects of plaque structure and material properties on stress distributions in human atherosclerotic plaques using 3D FSI models. Journal of Biomechanical Engineering 127 (7), 1185–1194.
Timmins, L.H., Wu, Q., Yeh, A.T., Moore, J.E., Greenswald, S.E., 2010. Structural inhomogeneity and fiber orientation in the inner arterial media. American Journal of Physiology—Heart and Circulatory Physiology 298, 1537–1545.
Tracqui, P., Broisat, A., Toczek, J., Mesnier, N., Ohayon, J., Riou, L., 2011. Mapping elasticity moduli of atherosclerotic plaque in situ via atomic force microscopy. Journal of Structured Biology 174 (1), 115–123.
Vaenkatesan, V., Li, Z.L., Vellinga, W.P., 2006. Adhesion and friction behaviours of polydimethylsiloxane—a fresh perspective on JKR measurements. Polymer 47 (25), 8317–8325.